# Should we correct the bias in Confidence Bands for Repeated Functional Data?

Emilie Devijver[1]     CNRS, Univ. Grenoble Alpes, Grenoble INP, LIG, 38000 Grenoble, France

Adeline Samson     Univ. Grenoble Alpes, CNRS, Grenoble INP, LJK, 38000 Grenoble, France

## Abstract

While confidence intervals for finite quantities are well-established, constructing confidence bands for objects of infinite dimension, such as functions, poses challenges. In this paper, we explore the concept of parametric confidence bands for functional data with an orthonormal basis. Specifically, we revisit the method proposed by Sun and Loader, which yields confidence bands for the projection of the regression function in a fixed-dimensional space. This approach can introduce bias in the confidence bands when the dimension of the basis is misspecified. Leveraging this insight, we introduce a corrected, unbiased confidence band. Surprisingly, our corrected band tends to be wider than what a naive approach would suggest. To address this, we propose a model selection criterion that allows for data-driven estimation of the basis dimension. The bias is then automatically corrected after dimension selection. We illustrate these strategies using an extensive simulation study. We conclude with an application to real data.

*Keywords:* functional data, repeated data, confidence band, Kac-Rice formulae, bias, dimension selection

# Contents

---
[1]Corresponding author: emilie.devijver@univ-grenoble-alpes.fr

# 1   Introduction

Functional data analysis is widely used for handling complex data with smooth shapes, finding applications in diverse fields such as neuroscience (e.g., EEG data, Zhang (2020)), psychology (e.g., mouse-tracking data, Quinton et al. (2017)), and sensor data from daily-life activities (Jacques and Samardžić (2022)).

We consider several independent observations of the same function, i.e. noisy functional data. To analyze this data, a classic approach involves projecting the data onto a functional space defined by a family of functions (Li, Qiu, and Xu (2022), Kokoszka and Reimherr (2017) Chapter 3). When the family is an orthonormal basis, e.g., the Legendre basis (with the standard scalar product) or Fourier (with another scalar product), the projection is explicit and it is possible to obtain theoretical results. However, some families, such as splines, are not orthonormal for the standard scalar product. We will discuss the impact of the choice of this family on estimation. We explain why the use of a  functional space offers a key advantage: it reduces the problem of inference to the estimation of coefficients, for example by least squares or maximum likelihood estimation. The function estimator is then simply an average after projection onto the functional base. It is important to accompany the function estimate with a measure of the uncertainty of that estimate, usually using confidence intervals or bands. In this paper, we focus on constructing a simultaneous confidence band for the mean of the function, rather than point-wise confidence intervals. This task presents several challenges: the confidence band must effectively control the simultaneous functional type-I error rate, as opposed to point-wise rates; it must strike a balance between being sufficiently conservative to maintain a confidence level while not being overly so as to render it meaningless; and the method used to construct this confidence band should be computationally feasible for practical application.

Several developments have already been proposed to answer these questions. First, let us consider the case of a single individual (no repetition) but with many time points. Some methods study the asymptotic distribution of the infinity norm between the true function and its estimator. The asymptotics in the number of time points is studied in Hall (1991), Claeskens and Van Keilegom (2003). This approach only works for large datasets in time and is likely to be too conservative otherwise. For small samples, bootstrap methods have been developed to compute the confidence band (Neumann and Polzehl (1998), Claeskens and Van Keilegom (2003)), but with a high computational cost. Another

approach is to construct confidence bands based on the volume of the tube formula. Sun and Loader (1994) studied the tail probabilities of suprema of Gaussian random processes. This approach is based on an unbiased linear estimator of the regression function. Zhou, Shen, and Wolfe (1998) used the volume-of-tube formula for estimation by regression splines. Krivobokova, Kneib, and Claeskens (2010) used this method for the construction of confidence bands by penalized spline estimators. They proposed to mix Bayesian and frequentist approaches, in order to obtain the good properties of the Bayesian world while reducing the variability to be less conservative using the frequentist approach. The bias is taken into account by spline modeling, assuming that enough knots are considered.

Some papers, like ours, rely on several observations of the same function. Liebl and Reimherr (2023) proposed a method based on the Kac-rice formula, random field theory and the volume-of-tube formula. They provide a band with locally varying widths using an unbiased estimator. Their method does not require estimation of the full covariance function of the estimator, but only its diagonal. This reduces the computational time. From a practical viewpoint, Sachs, Brand, and Gabriel (2022) introduced a package to popularize simultaneous confidence bands, in the context of survival analysis. Bunea, Ivanescu, and Wegkamp (2011) propose a threshold-type estimator and derive error bounds and simultaneous confidence bands, having an unbiased estimator. Telschow and Schwartzman (2022) propose a simultaneous confidence band based on the Gaussian kinematic formula. Again, it assumes access to an asymptotically unbiased estimator of the function of interest. The coverage will thus be guaranteed in the asymptotic setting after removing the bias, by smoothing the data for example. Their paper considers the non-gaussian and non-stationary cases. Wang (2022) proposed a simultaneous Kolmogorov-Smirnov confidence band by modeling the error distribution, thus avoiding the estimation of the covariance structure of the underlying stochastic process. They rely on B-splines for the estimation of the mean curve. Note that recent extensions have been proposed, based on Lipschitz-Killing-Curvatures estimators in Telschow et al. (2023), based on conformal prediction in Diquigiovanni, Fontana, and Vantini (2022), or having a prediction goal in mind in Hernández, Cugliari, and Jacques (2024) by considering functional time series data set.

One limitation of all those approaches is that they do not clearly take into account the bias of the functional estimator. Taking account of bias is particularly important when working in a non-asymptotic context. Sun and Loader (1994) proposed a bias correction for a particular class of functions but left the smoothing parameter choice open, leading to an unusable estimator. In the nonparametric framework, the bias is approximated using the estimator of the second derivative of the underlying mean function (Xia (1998)). But in general, there is a lack of discussion on how to handle the bias of the functional estimator, even in the simple case of a functional space of finite dimension.

Another issue is the selection of the dimension of the basis. Hard-thresholding approaches, cross-validation methods (Li, Qiu, and Xu (2022)) or model selection framework could be used to select the best dimension. However, these approaches need to be adapted to the specific case of controlling the level of a confidence band. Few references exist on this subject. For example, while the model selection paradigm has been extensively studied in the literature, in multivariate statistics or functional data analysis (e.g., Goepp, Bouaziz, and Nuel (2025), Aneiros, Novo, and Vieu (2022), Basna, Nassar, and Podgórski (2022)), it has not been explored in the context of confidence band construction.

The objective of this paper is to address the bias problem in confidence band construction for a general function, in the non-asymptotic setting, utilizing a finite functional orthonormal family and to select the best band. Our contributions are as follows:

- we disentangle the bias issue by explicitly defining the parameter of interest within the approach of Sun and Loader (1994);

- we propose a bias correction method in a new confidence band for the function of interest.

This provides a collection of debiased confidence bands. We also propose a criteria to select the best band, by splitting the sample into two sub-samples

- to avoid the loss of precision due to sample splitting, we propose a second heuristic method for selecting the dimension of the approximation space, treating it as a model selection problem, with a trade-off between conservatism and confidence level assurance; this approach does not correct the bias of each band of the collection but selects a band with a negligible bias;

- we illustrate the proposed strategies and compare them to cross-validation or threshold approaches;

- we also illustrate the impact of the choice of the functional family, including non-orthonormal families.

The paper is organized as follows: Section 2 introduces the functional regression model, the considered functional family and the corresponding approximate regression models, as well as an estimator defined in the finite space, along with descriptions of the error terms. In Section 3, we propose a confidence band for the approximate regression function in the space of finite dimension, where the dimension is fixed. Section 4 proposes a strategy to construct a confidence band for the true function. This last confidence band being too conservative, Section 5 introduces a model selection criterion to select the best confidence band, doing a trade-off between conservatism and confidence level assurance. Section 6 illustrates the different estimating procedures of the confidence band. Section 7 proposes an application on real data. Section 8 ends the paper by a conclusion and discussion of perspectives.

## 2 Statistical Model

In this paper, we consider time series as discrete measurements of functional curves. We first present the general functional regression model (Section 2.1) where the regression function belongs to a finite functional family of dimension $L^*$. In practice, this dimension $L^*$ is unknown and we will work on functional space of dimension $L$. The regression model on the finite family of functions is presented in Section 2.2, and an estimator is proposed in Section 2.3, with a description of the error terms.

In the rest of the paper, we consider the space $L^2([0,1])$ with its standard scalar product $< f_1, f_2 >= \int_0^1 |f_1(t)f_2(t)|dt$, for $f_1, f_2 \in L^2([0,1])$. The notation $Vect$ denotes the linear span.

### 2.1 Functional regression model

Let $y_{ij}$ be the measure at fixed time $t_j \in [a,b]$ for individual $i = 1, \ldots, N$, with $j = 1, \ldots, n$. The case with time observations dependent of the individuals is a natural extension of this case, but introduces a bias through the interpolation that is not easy to take into account. We restrict ourselves to $[a,b] = [0,1]$, without loss of generality. We assume these observations are discrete-time measurements of individual curves, which are independent and noisy realisations of a common function $f$ that belongs to a functional space. Thus for each individual $i$, we consider the following functional regression model

$$y_{ij} = f(t_j) + \varepsilon_{ij},$$

where $\varepsilon_{i.} = (\varepsilon_{i1}, \ldots, \varepsilon_{in})$ is the measurement noise assuming that the $\varepsilon_i$ are independent.

For each individual $i = 1, \ldots, N$, we denote $y_{i.} = (y_{i1}, \ldots, y_{in})$, $t_. = (t_1, \ldots, t_n)$ and $f(t_.) = (f(t_1), \ldots, f(t_n))$ the $n \times 1$ vectors of the observations, times and function $f$ evaluated in $t_.$, respectively. We also denote $\mathbf{y} = (y_{1.}, \ldots, y_{N.})$ the whole matrix of observations.

4

Let us introduce the functional space $\mathcal{S}^{L^*} = Vect((t \mapsto B_\ell^{L^*}(t))_{1 \leq \ell \leq L^*})$ with $L^*$ functions $(B_\ell^{L^*})_{1 \leq \ell \leq L^*}$ assumed to be linearly independent. Then, for any $f \in \mathcal{S}^{L^*}$, there exists a unique vector of coefficients $(\mu_\ell^{L^*})_{1 \leq \ell \leq L^*}$ such that, for all $t$, $f(t) = \sum_{\ell=1}^{L^*} \mu_\ell^{L^*} B_\ell^{L^*}(t)$. The regression function $f$ verifies the following assumption:

**Assumption 1.** The function $f$ belongs to the space $\mathcal{S}^{L^*}$ of dimension $L^*$. It is denoted $f^{L^*}$ and defined as:

$$f(t) = f^{L^*}(t) = \sum_{\ell=1}^{L^*} \mu_\ell^{L^*} B_\ell^{L^*}(t).$$

Many functional spaces are available in the literature, as Splines, Fourier or Legendre families. We introduce the following assumption:

**Assumption 2.** The functional family $(t \mapsto B_\ell^{L^*}(t))_{1 \leq \ell \leq L^*}$ is orthonormal with respect to the standard scalar product $< .,. >$.

Note that if Assumption 2 holds, one get $\mu_\ell^{L^*} = < f^{L^*}, B_\ell^{L^*} >$ for $\ell = 1, \ldots, L^*$. The Legendre family is orthonormal, the Fourier family is orthogonal for the standard scalar product (but not orthonormal), and the B-splines family is not orthogonal. We will illustrate the impact of using one family or the other.

We also consider a functional noise through the following assumption.

**Assumption 3.** The sequence $\varepsilon_i$ is functional and allows Karhunen-Loève $L^2$ representation: there exists a sequence of coefficients $(c_{i\ell})_{1 \leq \ell}$ such that

$$\varepsilon_{ij} = \sum_{\ell \geq 1} c_{i\ell} \phi_\ell(t_j),$$

where the functions $(\phi_\ell)_{1 \leq L}$ can be written through eigenvalues and eigenfunctions of the covariance matrix $cov(\varepsilon_{ij}, \varepsilon_{ij'})$. Practically, we assume this sum to be finite, as done for example in Chen and Song (2015): there exists $L^\varepsilon$ such that

$$\varepsilon_{ij} = \sum_{1 \leq L \leq L^\varepsilon} c_{i\ell} \phi_\ell(t_j),$$

We also assume that the coefficients are Gaussian: for all $i = 1, \ldots, N$ and $\ell = 1, \ldots, L^\varepsilon$,

$$c_{i\ell} \sim_{iid} \mathcal{N}(0, \sigma^2).$$

Assumption 1 and Assumption 3 imply that each curve $y_i$ belongs to a finite family: for $j = 1, \ldots, n$,

$$y_{ij} = \sum_{\ell=1}^{L^*} \mu_\ell^{L^*} B_\ell^{L^*}(t_j) + \sum_{\ell=1}^{L^\varepsilon} c_{i\ell} \phi_\ell(t_j).$$

As the observations are recorded at discrete time points $(t_j)_{1 \leq j \leq n}$, for $L \in \mathbb{N}$, let us denote $\mathbf{B}^L$ the matrix of $n \times L$ with coefficient in row $j$ and column $\ell$ equal to $B_\ell^L(t_j)$, and the basis for the noise $\Phi^{L^\varepsilon} = (\phi_\ell(t_j))_{1 \leq \ell \leq L^\varepsilon, 1 \leq j \leq n}$. Let us introduce $c_{i.} = (c_{i1}, \ldots, c_{iL^\varepsilon})$ the $L^\varepsilon \times 1$ vector. Then $\varepsilon_{i.} = \Phi^{L^\varepsilon} c_{i.}$. The vectors $y_{i.} \in \mathbb{R}^n$ are thus independent and $y_i \sim \mathcal{N}_n(f(t), \sigma^2 \Sigma^{L^\varepsilon})$ with $\Sigma^{L^\varepsilon} = \Phi^{L^\varepsilon}(\Phi^{L^\varepsilon})^T$.

The objective of this paper is to construct a tight confidence bound for $f^{L^*}$ using data $(y_{ij})_{ij}$. The main challenge is that the true dimension $L^*$ is unknown. In the rest of the paper, we will work with a collection of models defined on a finite family of dimension $L$ with $L \in \{L_{\min}, \ldots, L_{\max}\}$, $L_{\max}$ being chosen to be sufficiently large by the user, expecting that $L^* \leq L_{\max}$. $L_{\max}$ has to be large enough to

178 do overfitting. Then we will propose different strategies to choose the best bandwidth among the
179 different collections.

180 First, in Section 2.2 and Section 2.3, we define for a fixed $L$ the corresponding regression model and
181 its estimator. Then Section 3, Section 4 and Section 5 will introduce the different bandwidths.

## 2.2   Approximation of the model on a finite family

183 Let $f^{L^*} \in \mathcal{S}^{L^*}$ with $L^*$ unknown, and consider the space $\mathcal{S}^L$ for $L$ fixed in $\{L_{\min}, \dots, L_{\max}\}$. As $\mathcal{S}^L$
184 is a family of linearly independent functions, there is always a unique vector $\mu^{L,L^*}$ of coefficients
185 defining $f^{L,L^*}(t) = \sum_{\ell=1}^{L} \mu_\ell^{L,L^*} B_\ell^L(t) = B^L(t)\mu^{L,L^*}$ such that

$$f^{L,L^*} = \arg \min_{f \in \mathcal{S}^L} \{\|f^{L^*} - f\|_2^2\}.$$

186 If the family is orthonormal, it corresponds to the projected coefficients $\mu_\ell^{L,L^*}$:

$$\mu_\ell^{L,L^*} := <f^{L^*}, B_\ell^L> .$$

187 We can prove the following property:

**Proposition 2.1.** *Under Assumption 1,*

$$f^{L^*,L^*} = f^{L^*}.$$

189 *Moreover, if Assumption 2 also holds, the projection coefficients verify*

$$\mu_\ell^{L,L^*} = \mu_\ell^{L^*} \quad for \ \ell = 1, \dots, \min(L, L^*).$$

190 In practice, data are observed at discrete time, we consider the operator $\mathbf{P}^L$ defined as the matrix
191 $\mathbf{P}^L = ((\mathbf{B}^L)^T \mathbf{B}^L)^{-1}(\mathbf{B}^L)^T$ of size $L \times n$. This coincides with the orthogonal projection when we deal
192 with an orthonormal basis, but it is also consistent for non orthonormal family, coming back to the
193 least square estimator on a specified family. Then we define the coefficients $\underline{\mu}^{L,L^*}$ which are the
194 coefficients of $\mu^{L,L^*}$ approximated on the vector space, denoted $\mathbf{S}^L$, defined by the matrix $\mathbf{B}^L$.

$$\underline{\mu}^{L,L^*} := \mathbf{P}^L \mathbf{B}^{L^*} \mu^{L^*}.$$

195 The corresponding finite approximated regression function is denoted $\underline{f}^{L,L^*}$ and is defined, for all
196 $t \in [0, 1]$, as

$$\underline{f}^{L,L^*}(t) = B^L(t)\underline{\mu}^{L,L^*}.$$

197 We can prove the following properties linking $L, L^*$ and the number of timepoints $n$:

**Proposition 2.2.** *Under Assumption 1 and Assumption 2, the diagonal elements of $\mathbf{P}^L \mathbf{B}^{L^*}$ are such*
199 *that for $\ell = 1, \dots, \min(L, L^*)$,*

$$[\mathbf{P}^L \mathbf{B}^{L^*}]_{\ell\ell} = 1.$$

200  • *When $L \geq L^*$, when $n > L$, we have for $\ell = 1, \dots, L^*$,*

$$\underline{\mu}_\ell^{L,L^*} = \mu_\ell^{L^*}.$$

201  • *When $L < L^*$, for $\ell = 1, \dots, L$,*

$$\underline{\mu}_\ell^{L,L^*} \neq \mu_\ell^{L^*}.$$

6

202 • When $n \to \infty$, *for* $\ell = 1, \dots, L$

$$\underline{\mu}_\ell^{L,L^*} \to \mu_\ell^{L^*}.$$

203 • If $n > L^*$, then $f^{L^*} = f^{L^*,L^*} = \underline{f}^{L^*,L^*}.$

## 2.3 Estimator

205 Let $L \in \{L_{\min}, \dots, L_{\max}\}$. This section presents the least square estimator of the regression function
206 on the space of dimension $L$ defined by the family $\mathbf{B}^L$ and discusses its error.

### 2.3.1 Estimation of the regression function

208 When considering the estimation of the regression function $f^{L^*}$ on the space of dimension $L$ defined
209 by the family $\mathbf{B}^L$, we do not directly estimate $f^{L^*}$ but its projection on this finite space, which
210 corresponds to the projected function $\underline{f}^{L,L^*}(t)$ and its associated coefficients $(\underline{\mu}_\ell^{L,L^*})_{1 \le \ell \le L}$.

211 **Definition 2.1.** The vector of coefficients $(\underline{\mu}_\ell^{L,L^*})_{1 \le \ell \le L}$ is estimated by the least square estimator
212 $\hat{\underline{\mu}}^{L,L^*}$ defined as:

$$\hat{\underline{\mu}}^{L,L^*} := \frac{1}{N} \sum_{i=1}^N \mathbf{P}^L y_{i\cdot}.$$

213 For a fixed $t \in [0,1]$, the estimator of the function $\underline{f}^{L,L^*}(t)$ is defined by:

$$\hat{\underline{f}}^{L,L^*}(t) = \sum_{\ell=1}^L \hat{\underline{\mu}}_\ell^{L,L^*} B_\ell^L(t) = B^L(t)\hat{\underline{\mu}}^{L,L^*}. \tag{1}$$

214 Equation 1 directly implies that the estimator is thus the empirical mean of the functional approxi-
215 mation of each individual vector of observations. Because we work with least squares estimators, we
216 can easily study the error of estimation of $\hat{\underline{\mu}}^{L,L^*}$ and $\hat{\underline{f}}^{L,L^*}$.

217 **Proposition 2.3.** *Under Assumption 1 and Assumption 3, we have*

$$\hat{\underline{\mu}}^{L,L^*} \sim \mathcal{N}_L\left(\underline{\mu}^{L,L^*}, \frac{\sigma^2}{N}\Sigma_B^{L,L^\varepsilon}\right),$$

218 *where the $L \times L$ covariance matrix $\Sigma_B^{L,L^\varepsilon}$ is defined as $\Sigma_B^{L,L^\varepsilon} := \mathbf{P}^L \Sigma^{L^\varepsilon}(\mathbf{P}^L)^T$ with $\Sigma^{L^\varepsilon} = \Phi^{L^\varepsilon}(\Phi^{L^\varepsilon})^T$.*

219 *Moreover, $B^L()\mathbf{P}^L y_i$ is a Gaussian process with mean $\underline{f}^{L,L^*}()$ and covariance function $(s,t) \mapsto$*
220 *$\sigma^2 B^L(s)\Sigma_B^{L,L^\varepsilon}(B^L(t))^T$, and $(\hat{\underline{f}}^{L,L^*} - \underline{f}^{L,L^*})()$ is a centered Gaussian process with covariance function*
221 *$C^{L,L^*} : (s,t) \mapsto \frac{\sigma^2}{N} B^L(s)\Sigma_B^{L,L^\varepsilon} B^L(t)^T$.*

222 The proof is given in Appendix.

223 Even if the estimator $\hat{\underline{f}}^{L,L^*}$ is defined on the functional space associated to $\mathbf{S}^L$, it can also be seen as an
224 estimator of the function $f^{L^*}$ which lies in the space $\mathcal{S}^{L^*}$. In that case, the error includes a functional
225 approximation term due to the approximation of $f^{L^*}$ on the space $\mathcal{S}^L$, which will be nonzero if
226 $L \ne L^*$. It corresponds to the bias of the estimator $\hat{\underline{f}}^{L,L^*}$, i.e. the difference between its expectation
227 and the true $f^{L^*}$. Indeed, recalling that $f^{L^*} = \underline{f}^{L^*,L^*}$, the error of estimation can be decomposed into

$$\hat{\underline{f}}^{L,L^*}(t) - f^{L^*}(t) = \hat{\underline{f}}^{L,L^*}(t) - \underline{f}^{L,L^*}(t) + \underline{f}^{L,L^*}(t) - \underline{f}^{L^*,L^*}(t) =: Stat_{L,L^*}(t) + Bias_{L,L^*}(t), \tag{2}$$

7

228 The first term $Stat_{L,L^*}(t) = \underline{\overset{L,L^*}{\hat{f}}}(t) - \underline{f}^{L,L^*}(t)$ is the (unrescaled) statistics of the model. The second

229 term $Bias_{L,L^*}(t) = \mathbb{E}(\underline{\overset{L,L^*}{\hat{f}}}(t)) - \underline{f}^{L^*,L^*}(t)$ is the bias of the estimator $\underline{\overset{L,L^*}{\hat{f}}}(t)$ when estimating the true

230 function $\underline{f}^{L^*,L^*}(t)$.

231 Let us remark that this bias is different than the bias of the estimator $\overset{L,L^*}{\hat{f}}(t)$ when estimating the

232 projected function $\underline{f}^{L,L^*} = f^{L^*}$, which is 0. The two terms defined in Equation 2 are more detailed in

233 the two next subsections.

### 2.3.2  Statistics

235 The statistics of the model, $t \mapsto Stat_{L,L^*}(t) = \overset{L,L^*}{\hat{f}}(t) - \underline{f}^{L,L^*}(t)$, is a random functional quantity which

236 depends on the estimator $\overset{L,L^*}{\hat{f}}$. From Proposition 2.3, for any $t \in [0,1]$, we define the centered and

237 rescaled statistics $Z_L(t)$:

$$Z_L(t) := \frac{Stat_{L,L^*}(t)}{\sqrt{\mathrm{Var}(Stat_{L,L^*}(t))}} = \frac{\underline{\overset{L,L^*}{\hat{f}}}(t) - \underline{f}^{L,L^*}(t)}{\sqrt{C^{L,L^*}(t,t)}} \sim \mathcal{N}(0,1).$$

238 The covariance function can be naturally estimated using the observations $y_{i.}$ as

$$\hat{C}^{L,L^*}(s,t) = \frac{1}{N-1} \sum_{i=1}^{N} (B^L(s)\mathbf{P}^L y_{i.} - \underline{\overset{L,L^*}{\hat{f}}}(s))(B^L(t)\mathbf{P}^L y_{i.} - \underline{\overset{L,L^*}{\hat{f}}}(t)).$$

### 2.3.3  Bias

240 The bias is due to the fact that the estimation is potentially performed in a different (finite) space

241 than the space where the true function $\underline{f}^{L^*,L^*}$ lives. This is a functional bias, which is not random. It

242 corresponds to the approximation of $f^{L^*}$ from $\mathcal{S}^{L^*}$ to the space $\mathcal{S}^L$. It can be written as follows:

$$Bias_{L,L^*}(t) = B^L(t)\underline{\mu}^{L,L^*} - B^{L^*}(t)\mu^{L^*}.$$

243 Thus, when $L < L^*$ and the family is orthonormal, the approximation is the orthogonal projection

244 and we can deduce that

$$Bias_{L,L^*}(t) = \sum_{\ell=1}^{L} B_\ell^L(t)\underline{\mu}_\ell^{L,L^*} - \sum_{\ell=1}^{L^*} B_\ell^{L^*}(t)\underline{\mu}_\ell^{L^*} = \sum_{\ell=L+1}^{L^*} B_\ell^{L^*}(t)\underline{\mu}_\ell^{L^*}.$$

245 From Proposition 2.3, we can directly deduce the following proposition:

246 **Proposition 2.4.** *Under Assumption 1 and Assumption 3, the bias is, for all $t \in [0,1]$,*

247     • *for $L < L^*$, $Bias_{L,L^*}(t) \neq 0$,*

248     • *for $L \geq L^*$, $Bias_{L,L^*}(t) = 0$.*

249 In the next section, we explain how we use this property to derive confidence bands of $\underline{f}^{L,L^*}$ and

250 $f^{L,L^*}$.

8

# 3 Confidence Bands of $\underline{f}^{L,L^*}$ and $f^{L,L^*}$ for a fixed $L$

The objective is to construct a confidence band for the two functions $\underline{f}^{L,L^*}$ and $f^{L,L^*}$, based on the observations $\mathbf{y}$, for a given value $L \in \{L_{\min}, \dots, L_{\max}\}$. The band for $\underline{f}^{L,L^*}$ enters the framework proposed by Sun and Loader (1994) which relies on an unbiased and linear estimator of the function as the estimator $\underline{\hat{f}}^{L,L^*}$ is an unbiased estimator of $\underline{f}^{L,L^*}$. We recall in Section 3.1 the construction of this confidence band which attains a given confidence level in a non-asymptotic setting, that is for a finite number of observations $n$ for each individual. Then in Section 3.2, we prove that the confidence band proposed by Sun and Loader (1994) can be viewed as a confidence band for $f^{L,L^*}$ with an asymptotic confidence level, the asymptotic framework being considered when $n \to \infty$.

## 3.1 Confidence band for $\underline{f}^{L,L^*}$

Consider $1 - \alpha$ a fixed confidence level. The aim is to find a function $d^L()$ such that

$$\mathbb{P}\left(\forall t \in [0,1], \ \underline{\hat{f}}^{L,L^*}(t) - d^L(t) \leq \underline{f}^{L,L^*}(t) \leq \underline{\hat{f}}^{L,L^*}(t) + d^L(t)\right) = 1 - \alpha.$$

Consider the normalized statistics $Z_L(t)$ which is a centered and reduced Gaussian process. We want to find the quantile $q^L$ satisfying

$$q^L = \arg\min_q \left\{ \mathbb{P}\left( \max_{t \in [0,1]} |Z_L(t)| \leq q \right) = 1 - \alpha \right\}. \tag{3}$$

Then we can take $d^L(t) = q^L \sqrt{C^{L,L^*}(t,t)}$. The covariance function $C^{L,L^*}(t,t)$ can be replaced by its estimator $\hat{C}^{L,L^*}(t,t)$, making the distribution a Student's distribution with $N - 1$ degrees of freedom. Thus, it only requires to be able to compute the critical value $q^L$.

This can be done following Sun and Loader (1994) who propose a confidence band for a centered Gaussian process. Their procedure is based on an unbiased linear estimator of the function of interest, which is the case for $\underline{\hat{f}}^{L,L^*}$ when we consider a band for $\underline{f}^{L,L^*}$. We recall their result in the following proposition, the computation of the value $q^L$ is detailed thereafter.

**Theorem 3.1** (Sun and Loader (1994)). *Set Assumption 1 and Assumption 3 and a probability $\alpha \in [0,1]$. Then, we have*

$$\mathbb{P}\left(\forall t \in [0,1], \left|\underline{\hat{f}}^{L,L^*}(t) - \underline{f}^{L,L^*}(t)\right| \leq \hat{d}^L(t)\right) = 1 - \alpha$$

*with*

$$\hat{d}^L(t) = \hat{q}^L \sqrt{\hat{C}^{L,L^*}(t,t)/N}$$

*and $\hat{q}^L$ defined as the solution of the following equation, seen as a function of $q^L$:*

$$\alpha = \mathbb{P}\left(|t_{N-1}| > q^L\right) + \frac{\|\tau^L\|_1}{\pi}\left(1 + \frac{(q^L)^2}{N-1}\right)^{-(N-1)/2}, \tag{4}$$

*with $(\tau^L)^2(t) = \partial_{12}c(t,t) = Var(Z_L(t))'$ where we denote $\partial_{12}c(t,t)$ the partial derivatives of a function $c(t,s)$ in the first and second coordinates and then evaluated at $t = s$.*

9

We can thus deduce a confidence band of level $1 - \alpha$ for $\underline{f}^{L,L^*}$:

$$CB_1(\underline{f}^{L,L^*}) = \left\{ \forall t \in [0,1], \left[ \underline{\hat{f}}^{L,L^*}(t) - \hat{d}^L(t); \underline{\hat{f}}^{L,L^*}(t) + \hat{d}^L(t) \right] \right\}.$$

The value $\hat{q}^L$ is defined implicitly in Equation 4 which involves the unknown and not explicit quantity $t \mapsto \tau^L(t)$. Liebl and Reimherr (2023) propose to estimate $\hat{\tau}^L(t)$, for all $t$, by

$$\hat{\tau}^L(t) = \left( \widehat{Var}((U^L)'_1(t), \ldots, (U^L)'_N(t)) \right)^{1/2}$$

$$= \left( \frac{1}{N-1} \sum_{i=1}^N \left( (U^L)'_i(t) - \frac{1}{N} \sum_{j=1}^N (U^L)'_j(t) \right)^2 \right)^{1/2},$$

where $U_i^L(t) = (P^L y_i(t) - \underline{\hat{f}}^{L,L^*}(t))/(\hat{C}^{L,L^*}(t))^{1/2}$ and $(U^L)'_i$ is a smooth version of the differentiated function $U_i^L$. Then we take the $L_1$-norm of $\hat{\tau}^L$.

Let us describe the behavior of $\hat{d}^L$:

- $\|\hat{d}^L\|_\infty$ increases with $L$.
- When the functions $(B_\ell^L)_{1 \le \ell \le L}$ form an orthonormal family, $\|\hat{d}^L\|_\infty$ increases with $L$ until $L = L^*$ and then $\|\hat{d}^L\|_\infty$ is constant with $L$.

Their behavior will be illustrated with different function families in Section 6.

## 3.2 Asymptotic confidence band for $f^{L,L^*}$

Note that in the asymptotic framework $n \to \infty$, the previous definition of $\hat{d}^L$ induces a natural asymptotic confidence band for the function $f^{L,L^*}$. Indeed, we can prove that

**Theorem 3.2.** *Set Assumption 1 and Assumption 3 and a probability $\alpha \in [0,1]$. Then, we have,*

$$\lim_{n \to +\infty} \mathbb{P} \left( \forall t \in [0,1], |\underline{\hat{f}}^{L,L^*}(t) - f^{L,L^*}(t)| \le \hat{d}^L(t) \right) = 1 - \alpha,$$

*with $\hat{d}^L(t) = \hat{q}^L \sqrt{\hat{C}^{L,L^*}(t,t)/N}$ and $\hat{q}^L$ is defined as the solution of Equation 4.*

The proof is given in Appendix.

Then a confidence band for $f^{L,L^*}$ at the asymptotic confidence level $1 - \alpha$ for a large number of observations $n$ is given by

$$CB(f^{L,L^*}) = \left\{ \forall t \in [0,1], \left[ \underline{\hat{f}}^{L,L^*}(t) - \hat{d}^L(t); \underline{\hat{f}}^{L,L^*}(t) + \hat{d}^L(t) \right] \right\}.$$

## 4  Confidence Band of $f^{L^*}$ by correcting the bias

The function of interest is $f^{L^*} = \underline{f}^{L^*,L^*}$, rather than $\underline{f}^{L,L^*}$. Therefore, our objective is to construct a confidence band for $f^{L^*}$. However, an unbiased estimator of $f^{L^*}$ is not available by definition, since the true dimension $L^*$ is unknown. We propose instead to work with the estimator $\underline{\hat{f}}^{L,L^*}$ and to debias the corresponding confidence band.

To do this, we use the decomposition between the bias term and the statistical term, outlined in Equation 2. The idea is to bound the infinite norm of these two terms. A first strategy is to bound

10

each term separately, then add the two bounds to construct the confidence band. However, this approach tends to produce a band that is too large and too conservative. This is because applying the infinite norm to each term before bounding them does not take into account the functional nature of the two terms.

A second strategy is to retain the functional aspect by bounding the infinity norm of the sum of the two functional terms. This approach is detailed in this section. In Section 4.1, we first rewrite the band as a band around $\underline{f}^{L,L^*}(t)$. We need to estimate the band bound and the bias. To do this, we divide the sample into two sub-samples. This choice is not ideal because it increases the variability of the estimators. But at least, it provides independence between the estimators of the two quantities, which makes it possible to establish the theoretical coverage of the final band. More precisely we use a first subsample $\mathbf{y}^1$ to estimate the bound defined in Section 3. A second subsample $\mathbf{y}^2$ is used to estimate the bias term (without the infinite norm). This results in a pointwise correction of the bias, and the final confidence band is centered around $\underline{f}^{L_{\max},L^*}$. This procedure provides a collection of confidence bands, for $L \in \{L_{\min}, \dots, L_{\max}\}$ with variable width. Then, in Section 4.2, we propose a criterion to select the "best" band by minimizing its width. We discuss the band thus obtained at the end of the section and its limits.

## 4.1 Construction of the band of $f^{L^*}$ for a given $L$

We introduce two independent sub-samples $\mathbf{y}^1$ and $\mathbf{y}^2$ of $\mathbf{y}$ of length $N_1$ and $N_2$ such that $N_1 + N_2 = N$.

We use the first sub-sample $\mathbf{y}^1$ to calculate $\underline{\hat{f}_1}^{L,L^*}(t)$, an estimator of $\underline{f}^{L,L^*}(t)$ and a functional bound denoted $\hat{d}_1^L$ that controls the bias term $\underline{f}^{L,L^*}(t) - \underline{\hat{f}_1}^{L,L^*}(t)$. This bound is defined in Section 3 applied on $\mathbf{y}^1$, for a given level $\alpha$, such that:

$$\mathbb{P}\left(\forall t \in [0,1], -\hat{d}_1^L(t) \leq \underline{f}^{L,L^*}(t) - \underline{f}_1^{L,L^*}(t) \leq \hat{d}_1^L(t)\right) = 1 - \alpha. \tag{5}$$

Next, we need to control the bias $Bias_{L,L^*}(t) = \underline{f}^{L,L^*}(t) - f^{L^*}(t)$. Recall that when $L_{\max}$ is sufficiently large and $n > L_{\max}$, we have $f^{L^*} = \underline{f}^{L_{\max},L^*}$. We therefore need to control the $Bias_{L,L^*}(t) = \underline{f}^{L,L^*}(t) - \underline{f}^{L_{\max},L^*}(t)$. It would be tempting to replace $Bias_{L,L^*}(t)$ by its estimation based on the second sample $\mathbf{y}^2$. But this would introduce an estimation error that we also need to control, in the same spirit as what is done in Lacour, Massart, and Rivoirard (2017). We can again use Section 3 to compute the function $\hat{d}_2^{L,L_{\max}}(t)$ on the sample $\mathbf{y}^2$, and the functional estimators $\underline{f}_2^{L,L^*}(t)$ and $\underline{f}_2^{L_{\max},L^*}(t)$ of $\underline{f}^{L,L^*}(t)$ and $\underline{f}^{L_{\max},L^*}(t)$, respectively. This allows us to construct the following band for $\underline{f}^{L,L^*}(t) - \underline{f}^{L_{\max},L^*}$ for a confidence level $1 - \beta$,

$$\mathbb{P}\left(\forall t \in [0,1], -\hat{d}_2^{L,L_{\max}}(t) \leq \underline{f}^{L_{\max},L^*}(t) - \underline{f}^{L,L^*}(t) - (\underline{f}_2^{L_{\max},L^*}(t) - \underline{f}_2^{L,L^*}(t)) \leq \hat{d}_2^{L,L_{\max}}(t)\right) = 1 - \beta. \tag{6}$$

Combining Equation 5 and Equation 6, we can provide a debiased confidence band of $f^{L^*}(t)$.

**Proposition 4.1.** *Let us define*

$$\hat{\theta}_1^L(t) := -\hat{d}_1^L(t) - \hat{d}_2^{L,L_{\max}}(t) + \underline{f}_2^{L_{\max},L^*}(t) - \underline{f}_2^{L,L^*}(t)$$

$$\hat{\theta}_2^L(t) := \hat{d}_1^L(t) + \hat{d}_2^{L,L_{\max}}(t) + \underline{f}_2^{L_{\max},L^*}(t) - \underline{f}_2^{L,L^*}(t),$$

11

where $\hat{d}_1^L(t)$ is defined on sample $\mathbf{y}^1$ by Equation 5 for a level $\alpha$ and $\hat{d}_2^{L,L_{\max}}(t)$ is defined on sample $\mathbf{y}^2$ by Equation 6 for a level $\beta$. Then we have

$$\mathbb{P}\left(\forall t \in [0,1], \quad \hat{\theta}_1^L(t) \leq f^{L^*}(t) - \underline{\hat{f}}_1^{L,L^*}(t) \leq \hat{\theta}_2^L(t)\right) \geq 1 - \alpha\beta.$$

The proof is given in Appendix.

This defines a confidence band which can be defined either around $\underline{\hat{f}}_1^{L,L^*}$:

$$CB_2(\underline{f}^{L^*}) = \left\{\forall t \in [0,1], \left[\underline{\hat{f}}_1^{L,L^*}(t) + \hat{\theta}_1^L(t)\,;\, \underline{\hat{f}}_1^{L,L^*}(t) + \hat{\theta}_2^L(t)\right]\right\}$$

or around $\underline{\hat{f}}_2^{L_{\max},L^*}$:

$$CB_2(\underline{f}^{L^*}) = \left\{\forall t \in [0,1], \left[\underline{\hat{f}}_2^{L_{\max},L^*}(t) + \bar{\theta}_1^L(t)\,;\, \underline{\hat{f}}_2^{L_{\max},L^*}(t) + \bar{\theta}_2^L(t)\right]\right\}.$$

with $\bar{\theta}_1^L(t) = \underline{\hat{f}}_1^{L,L^*}(t) - \underline{\hat{f}}_2^{L,L^*}(t) - \hat{d}_1^L(t) - \hat{d}_2^{L,L_{\max}}(t)$ and $\bar{\theta}_2^L(t) = \underline{\hat{f}}_1^{L,L^*}(t) - \underline{\hat{f}}_2^{L,L^*}(t) + \hat{d}_1^L(t) + \hat{d}_2^{L,L_{\max}}(t)$.

*Remark* 4.1. The two functions $\hat{d}_1^L(t)$ and $\hat{d}_2^{L,L_{\max}}(t)$ are of the same order because they are constructed using the same approach. They depend on the length of the samples. To obtain the thinnest band, the best strategy is to divide the sample in two sub-samples of equal length $N_1 = N_2 = N/2$.

The behavior of $\hat{d}_1^L$ was described in Section 3. Let us describe the behavior of $\hat{d}_2^{L,L_{\max}}$:

- $\|\hat{d}_2^{L,L_{\max}}\|_\infty$ decreases with $L$.
- When $L > L^\varepsilon$, $\|\hat{d}_2^{L,L_{\max}}\|_\infty$ is constant with $L$ and the probability in Equation 6 is equal to 1.
- When $L^* < L < L^\varepsilon$, $\|\hat{d}_2^{L,L_{\max}}\|_\infty$ is constant with $L$ when the functions $B_\ell^L$ form an orthonormal family. Otherwise, the behavior is erratic.

This means that when the band defined in Proposition 4.1 is calculated for $L > L^\varepsilon$, the confidence level is $1 - \alpha$ instead of $1 - \alpha\beta$.

The advantage of this approach is that the band bias is corrected and the level for the true function $f^{L^*}$ is guaranteed when $L^\varepsilon$ is large. This was the main aim of the paper. The main limit of this approach is that the band is constructed with samples with half sizes, leading to less precision. This will be illustrated in Section 6. Nevertheless, this method gives finer confidence bands than cross-validation, and with the right level of confidence.

A natural question is then the choice of the dimension $L$. This is the purpose of the next section.

## 4.2 Influence of $L$

This approach produces a collection of debiased confidence bands for different values of $L$. The confidence bands have different widths but a same confidence level $1 - \alpha\beta$. It is therefore natural to want to select one of them. This means that we want to select the best dimension $L$ among the collection $\{L_{\min}, \dots, L_{\max}\}$. We need to define what "best" means. It is quite intuitive to want on the finest band, fine in the sense of a certain norm. Here we consider the infinite norm of the width of the confidence band. This gives preference to smooth bands. We therefore define the following criteria of selection of $L$

$$\hat{L} = \arg\min_L \left\{\sup_t |\hat{\theta}_2^L(t) - \hat{\theta}_1^L(t)|\right\} = \arg\min_L \left\{\sup_t |\hat{d}^L(t) + \hat{d}^{L,L_{\max}}(t)|\right\}. \tag{7}$$

12

This global approach guarantees that each band of the collection is debiased and then the dimension is selected. It will be illustrated in Section 6.

In the next section, instead of debiasing each band, we employ another strategy focusing on the construction of a selection criteria that will guarantee that the bias is negligible.

# 5 Selection of the best confidence band with a criteria taking into account the bias

In this section, we want to use the collection of confidence bands defined in Section 3 without correcting their bias, but by proposing a selection criterion that is a trade-off between this bias and the dimension of the basis. To do this, we propose a new heuristic criterion linked to the definition of the band itself, considering the estimation of the band as the estimation of a quantile of a certain empirical process. The criterion is inspired by model selection tools for choosing the best dimension $L$. In the following, we assume that $L_{\max}$ is large enough such that $\underline{f}^{L_{\max}, L^*} = f^{L^*}$.

We work on the quantile $q^L$ introduced in Equation 3, its oracle version $q^{L^*}$ for level $L^*$ and its estimate $\hat{q}^L$. All are scalars, belonging to a collection indexed by $L = L_{\min}, \dots, L_{\max}$. A natural criterion for choosing the best $L$ is that the estimator $\hat{q}^L$ minimizes the quadratic error $\mathbb{E}\left(\|q^{L^*} - \hat{q}^L\|^2\right)$. However, this quadratic error is unknown as $q^{L^*}$ is unknown. We can not use it directly.

Instead, we study $\|\hat{q}^{L_{\max}} - \hat{q}^L\|^2$. While the theoretical quadratic error $\mathbb{E}\left(\|q^{L^*} - \hat{q}^L\|^2\right)$ decreases when $L < L^*$ and increases when $L > L^*$, the $\|\hat{q}^{L_{\max}} - \hat{q}^L\|^2$ approximation to this error always decreases when $L > L^*$, as illustrated in Section 6.

We see a behavior similar to a bias, high when the dimension is small, and small when the dimension is large. Selecting a dimension using this criterion will always overfit the data. We therefore propose to penalize this quantity by the dimension $L$ divided by the sample size $N$, as usual in model selection criterion. To do this we introduce a regularisation parameter $\lambda > 0$ which balances the two terms. A natural criteria to select the best $L$ is then

$$\widetilde{crit}(L) = \|\hat{q}^{L_{\max}} - \hat{q}^L\|^2 + \lambda \frac{L}{N}.$$

Then we define

$$\tilde{L} = \arg\min_L \widetilde{crit}(L),$$

and take the band centered around $\underline{f}^{\tilde{L}, L^*}$:

$$CB_3(\underline{f}^{L^*}) = CB_1(\underline{f}^{\tilde{L}, L^*})$$

This criterion is illustrated in Section 6.4. We also compare with two other standard approaches, heuristic as well, namely the cross-validation approach used to select the dimension $L$ which minimizes the reconstruction error, and a thresholding method which keeps the higher dimension $L$ with large enough coefficients. These two methods are less oriented to the objective of controling the level of the selected confidence band.

# 6 Simulation study

In this section, we illustrate the different statements provided along the paper on generated data. First, in Section 6.1, we describe the generating data process and illustrate the linear estimator considered

13

in this paper. In Section 6.2, we illustrate the first confidence band, for a fixed level, as introduced in
Section 3. Then, we illustrate the debiased confidence band in Section 6.3, and discuss the model
selection criterion in Section 6.4. We finally study the generalization of the method out of the class
of models in Section 6.5.

## 6.1 Generating data process

To illustrate the model, we simulate a regression functional model with $n = 50$ points per individual
and $N = 40$ individuals. In Figure 1, the function $f$ (red curve) belongs to the Fourier (resp. Legendre
and Spline) family with $L^* = 11$ and the noisy observations $y_{ij}$ (black curves) have a functional noise
in dimension $L^\varepsilon = 20$, also in the Fourier (resp. Legendre and Spline) family on the left plot (resp.
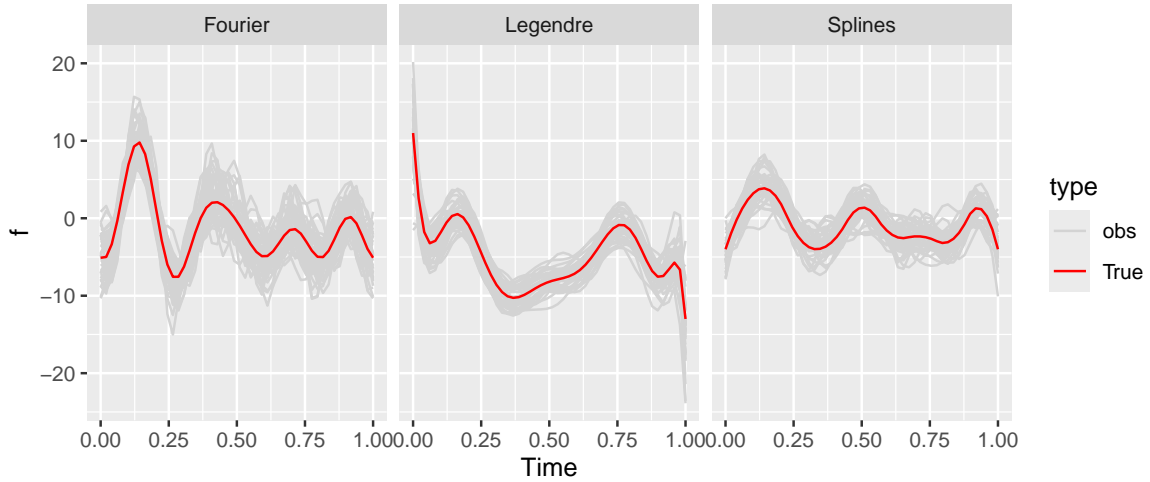middle and right).



Figure 1: Illustrative example. We generate a regression functional model in the Fourier (left),
Legendre (middle) and Splines (right) families. The red curve corresponds to the true function, and
the gray curves correspond to noisy observations.

Proposition 2.1 and Proposition 2.2 are illustrated in Appendix.

## 6.2 Confidence band for a fixed level

The band derived in Theorem 3.1 is illustrated on Figure 2. It displays on the top row several
functional data generated under either the Fourier family (left), Legendre (middle) or Spline (right),
on the middle row the confidence bands of $\underline{f}^{L,L^*}$ for different values of $L = 3, 5$ and $11$, and on the
bottom row the bound $\hat{d}^L$. The true functions $\underline{f}^{L,L^*}$ are displayed in cyan and the confidence bands in
purple. The bands are very precise for each $L$. The behavior of $\hat{d}^L$ increases with $L$. As $d^L$ can be
seen as a variance, $\hat{d}^L(t)$ is larger on the boundary of the time domain, as there are less observations
near 0 and 1.

We also evaluate numerically the levels of the obtained confidence bands. For this, 1000 datasets
are simulated, the confidence band is estimated for each of them. The empirical confidence level is
then evaluated as the proportion of confidence bands that contain the true function. Table 1 presents
the empirical confidence levels for different values of $L$ and two sample sizes $n = 50$ and $n = 150$,
with $N = 10$, $N = 40$ and $N = 60$. When $N = 40$ and $N = 60$, the level is the expected one whatever
the value of $L$, especially when $L < L^*$ and $N = 40$, but also when $L > L^\varepsilon$. We will see in the next
sections that this will not be the case for the debiased confidence band. When $N = 10$, the level is

14

too small, especially when $L$ is large. This might be due to the the large number of parameters to be
estimated in the covariance matrix $C$, with a small number of observations $N$.



Figure 2: Illustrative example. For the three families, resp. Fourier, Legendre and the splines, we display on the top row the observed functional data, on the middle row the confidence bands for different values of L (3, 5 and 11), and on the bottom row the bound dL.

## 6.3 Confidence bands by correcting the bias

We illustrate the results given in Proposition 4.1. In Figure 3, top row, we plot the confidence bands obtained for different dimensions $L \in \{3, 5, 11, 15, 21\}$ with Fourier, Legendre and Splines families and $\alpha = \beta = \sqrt{0.05} \approx 0.22$. We can see that all the confidence bands are alike. Especially, they are unbiased, even for $L = 3$. A larger dimension $L$ provides a smoother band. On the middle and bottom rows of Figure 3, we illustrate the two terms that enter the confidence band, $t \mapsto \hat{d}_1^L(t)$ and $t \mapsto \hat{d}_2^{L,L_{\max}}(t)$. Their behavior is the same along time. The function $\hat{d}_1^L(t)$ can be seen as a variance, this is why it is larger near 0 and 1 where there are less observations. The function $\hat{d}_2^{L,L_{\max}}(t)$ is smaller than $\hat{d}_1^L(t)$ because it controls the remaining rest after the projection. Note that as expected

15

Table 1: The confidence level of the confidence band CB is evaluated from 1000 repetitions. Confidence bands are calculated with the Fourier family (a), Legendre family (b) and Splines family (c), for several L in rows and several n and N in columns, for alpha = 0.05.

| L | n/N | | | | | |
|---|---|---|---|---|---|---|
|   | 50/10 | 150/10 | 50/40 | 150/40 | 50/60 | 150/60 |
| 3 | 0.920 | 0.922 | 0.949 | 0.949 | 0.948 | 0.951 |
| 5 | 0.915 | 0.913 | 0.951 | 0.952 | 0.944 | 0.942 |
| 11 | 0.896 | 0.895 | 0.941 | 0.944 | 0.945 | 0.945 |
| 15 | 0.886 | 0.879 | 0.940 | 0.940 | 0.944 | 0.941 |
| 21 | 0.918 | 0.906 | 0.949 | 0.949 | 0.950 | 0.949 |
| 25 | 0.918 | 0.906 | 0.949 | 0.949 | 0.950 | 0.949 |

| L | n/N | | | | | |
|---|---|---|---|---|---|---|
|   | 50/10 | 150/10 | 50/40 | 150/40 | 50/60 | 150/60 |
| 3 | 0.916 | 0.920 | 0.945 | 0.949 | 0.949 | 0.951 |
| 5 | 0.905 | 0.907 | 0.950 | 0.949 | 0.953 | 0.957 |
| 11 | 0.901 | 0.903 | 0.939 | 0.945 | 0.933 | 0.949 |
| 15 | 0.897 | 0.902 | 0.946 | 0.955 | 0.943 | 0.956 |
| 21 | 0.893 | 0.884 | 0.946 | 0.946 | 0.937 | 0.945 |
| 25 | 0.893 | 0.884 | 0.946 | 0.946 | 0.937 | 0.945 |

| L | n/N | | | | | |
|---|---|---|---|---|---|---|
|   | 50/10 | 150/10 | 50/40 | 150/40 | 50/60 | 150/60 |
| 3 | 0.910 | 0.906 | 0.935 | 0.936 | 0.941 | 0.943 |
| 5 | 0.891 | 0.891 | 0.949 | 0.947 | 0.947 | 0.952 |
| 11 | 0.899 | 0.901 | 0.941 | 0.948 | 0.942 | 0.942 |
| 15 | 0.910 | 0.903 | 0.942 | 0.940 | 0.937 | 0.940 |
| 21 | 0.912 | 0.911 | 0.937 | 0.943 | 0.939 | 0.945 |
| 25 | 0.909 | 0.907 | 0.939 | 0.939 | 0.950 | 0.948 |

when $L > L^\varepsilon$, $\hat{d}_2^{L,L_{\max}}(t)$ is close to 0. As explained before, the influence of $L$ is not the same for the two functions. When $L$ increases, $\hat{d}_1^L(t)$ increases while $\hat{d}_2^{L,L_{\max}}(t)$ decreases.



Figure 3: Illustrative example. For a given dataset, we plot several confidence bands (top row), functions dL (middle row) and dLLmax (bottom row). Bands and functions are estimated with Fourier (left column), Legendre (middle column) and Spline (right column) basis and several dimensions L (3, 5, 11, 15, 21).

In Table 2, we simulate 1000 repeated datasets with the Legendre family and with two sample sizes $n = 50$ and $n = 150$ and $N = 40$. For each dataset, we compute the confidence band defined in Proposition 4.1 with a theoretical confidence level of $1 - \alpha\beta = 0.95$ and for different values of $L$. Then the confidence level is approximated as the proportion of confidence bands containing the true function $f$. Remark that when $L < L^\varepsilon$, the level is the expected one, that is 0.95. When $L > L^\varepsilon$, the level is not more ensured, as explained before. Indeed the term $d^{L,L^{\max}}$ is mainly equal to 0, and the level is close to $1 - \alpha$ instead of $1 - \alpha\beta$. This is not the case for the band in Section 3, as this is due to the correction of the bias.

We illustrate the different terms involved in Equation 7. In Figure 4, we plot for a given dataset,

Table 2: Illustrative example. We display the level of confidence for the proposed confidence band CB2, for several L in rows and several n in columns, N=40, for alpha=0.2 and beta=0.2 (and then in total the confidence band reaches the level 0.95), and considering the Legendre family.

| L | n | |
|---|---|---|
| | 50 | 150 |
| 3 | 0.946 | 0.941 |
| 5 | 0.961 | 0.958 |
| 11 | 0.961 | 0.970 |
| 15 | 0.944 | 0.957 |
| 21 | 0.787 | 0.790 |
| 25 | 0.787 | 0.790 |

the infinity norm of the width of the band $\hat{d}^L(t) + \hat{d}^{L,L_{\max}}(t)$ (top), of $\hat{d}^L(t)$ (middle) and $\hat{d}^{L,L_{\max}}(t)$ (bottom) functions obtained with the Fourier (left column), Legendre (middle column) and Spline (right column) basis. As already said, $\|\hat{d}^L\|_\infty$ increases with $L$ while $\|\hat{d}^{L,L_{\max}}\|_\infty$ decreases (and is zero when $L > L^\varepsilon$). The width of the band wrt $L$ does not have a $U$-shape, as expected. It is thus difficult to minimize this criterion and the selection of $\hat{L}$ is thus not stable. But again, whatever the value of $\hat{L}$, the corresponding band is debiased in the collection. We will see in the next section that its width is smaller than standard approaches. The performance of the selection is also illustrated in the next section.



Figure 4: Illustrative example. For a given dataset, we calculate the norm of the width of the confidence band (top), of the dL function (middle) and the dLLmax function (bottom), for several dimensions L and for Fourier (left column), Legendre (middle column) and Splines (right column) basis.

## 6.4 Model selection criterion

We want to evaluate the performance of the two selection criteria introduced in this paper.

First, we consider the second approach presented in @sec-modsel. In Figure 5, we illustrate the

Table 3: Illustrative example. We display the level of confidence over 100 repetitions for the proposed confidence band CB3, for several model selection criterion in rows and several basis in columns, for alpha=0.05.

| model | Legendre | Fourier | Splines |
|-------|----------|---------|---------|
| L hat  | 0.89 | 0.72 | 0.81 |
| Lmax   | 0.92 | 0.94 | 0.91 |
| Lstar  | 0.92 | 0.90 | 0.92 |
| Ltilde | 0.93 | 0.96 | 0.37 |
| L.CV   | 0.94 | 0.91 | 0.92 |
| L.L0   | 0.98 | 0.93 | 0.92 |

behavior of the selection criterion introduced in Section 5 on simulated data, with $\lambda = 1$ for the three basis. We can see that $\tilde{L}$ is overestimated. When considering nested spaces, it ensures that $\tilde{L}$ tends to be larger than $L^*$ and thus the confidence band is automatically unbiased.



Figure 5: Illustrative example. For a given simulated dataset, we show the behavior of the criteria as a function of dimension L, for several lambdas, for Fourier (left), Legendre (middle) and Splines (right) basis.

We compare the two strategies $CB_2$ and $CB_3$ with some standard approaches. More precisely, we simulate 100 repeated datasets. The different confidence bands and the norm of their widths are computed for several $L$. We apply the selection criteria and plot the distribution of the estimated dimension in Figure 6, for the three basis families, for several model selection criteria: $\hat{L}$, $\tilde{L}$, cross validation and hard thresholding. The dimension $\hat{L}$ is almost always larger than the true $L^* = 11$. The fact that it is larger is not a problem because the selected band is unbiased and has the correct level as soon as $L^\varepsilon$ is large. However, the criterion tends to select a band that is (too) smooth. We can see that the selected dimension $\tilde{L}$ is smaller in distribution, and closer to the true value than $\hat{L}$. In addition, as we then use the confidence band of Section 3, the confidence level is guaranteed to be as expected. The model selected by cross validation is rather good, for all the basis considered. On the other hand, the model selected by hard thresholding is not good, particularly for a non orthonormal basis, which makes sense in relation to Proposition 2.1.

The reformulation of the band around $\hat{f}_2^{L_{\max}, L^*}$ is close to the band presented in Section 3 for

19

Figure 6: Illustrative example with $N = 40$. From 100 datasets, we calculate the distribution of the estimated dimension L, for four model selection criteria: from top to bottom, the debiased band proposed in CB2 with Lhat, the band CB3 with Ltilde, the cross validation and hard thresholding methods. The true dimension is $L^* = 11$.

$L = L_{\max}$, that is a band centered around $\underline{\hat{f}}^{L_{\max},L^*}$. A natural question is to understand what is the gain by doing so instead of using the band from Section 3 with $L = L_{\max}$, namely the band $\left[\underline{\hat{f}}^{L_{\max},L^*}(t) - \hat{d}^{L_{\max}}(t); \underline{\hat{f}}^{L_{\max},L^*}(t) + \hat{d}^{L_{\max}}(t)\right]$. To do that, we have to understand the behavior of the different terms. As it is difficult to compare theoretically the width of the two bands, we compare them using simulations. For 100 repeated datasets, we compute several confidence bands: the $CB_1$ band constructed in Section 3 with $L_{\max}$, the $CB_2$ band defined in Proposition 4.1 with $\hat{L}$, the $CB_3$ band defined in Section 5 with $\tilde{L}$ and the ideal (and not accessible) band constructed in Section 3 with the true $L^*$. In Figure 7, we present boxplots of the norms of the band width with $\hat{L}, L_{\max}, L^*$ and $\tilde{L}$. The width of the confidence band with the true $L^*$ is smaller, which is expected but unfortunately not achievable. The width of the confidence band $CB_1$ is smaller than that of the band $CB_2$. This can be explained by the fact that we estimate two different quantities, on smaller datasets, for more conservative levels ($1 - \alpha$ and $1 - \beta$ respectively) in order to finally achieve the confidence level of $1 - \alpha\beta$. This also explains why the cross validation and hard-thresholding methods, which also divide the sample into two parts, do not give good results either. The model given by the heuristic model selection criterion $\tilde{crit}$ achieves good performance. Note that the width of the selected model $\tilde{L}$ is better than the width of the confidence band with a large level $L_{\max}$, which one should have used to avoid model selection.



Figure 7: Illustrative example. We display within boxplots the confidence band's width over 100 repetitions for the dimension selected by the several criterion introduced in this paper, for Fourier (left), Legendre (middle) and Splines (right) basis.

### 6.5 Generalization out of the model

We now illustrate the behaviour of the bands when the basis used for estimation is poorly specified. We simulate 1000 data sets with a spline basis and estimate the confidence bands with the Fourier and Legendre basis, for different values of $n$ and $N$. The coverage rates are presented in Table 4. The Fourier basis does not give a correct rate. On the other hand, the Legendre basis gives very satisfactory coverage rates for $L > 20$.

Next, we illustrate the $\tilde{L}$ dimension selection method and compare it to the cross-validation method. Table 5 presents the coverage rates of the corresponding confidence bands estimated with the Fourier and Legendre basis, in the case $N = 40$ and $n = 150$. Once again, we see that the Fourier basis does not give good results, either by cross-validation or by $\tilde{L}$. On the other hand, with the Legendre basis, the $\tilde{L}$ method gives a satisfactory coverage rate, even if it is underestimated, whereas the cross-validation method is very poor. Moreover, the widths of the confidence bands selected with $\tilde{L}$ and by cross validation are represented by boxplot in Figure 8. It can be seen that the cross-validation approach

21

Table 4: Illustrative example. The confidence level of the confidence band is evaluated from 1000 repetitions. Data is generated using a Splines basis, and confidence bands are calculated with the Fourier (a) and Legendre (b) families, for several L in rows and several n and N in columns.

| L | n/N | | | |
|---|---|---|---|---|
| | 50/10 | 150/10 | 50/40 | 150/40 |
| 5 | 0.001 | 0.001 | 0.000 | 0.000 |
| 11 | 0.134 | 0.120 | 0.026 | 0.025 |
| 15 | 0.231 | 0.197 | 0.050 | 0.039 |
| 21 | 0.316 | 0.286 | 0.093 | 0.074 |
| 25 | 0.346 | 0.305 | 0.121 | 0.087 |
| 31 | 0.384 | 0.335 | 0.187 | 0.123 |
| 35 | 0.406 | 0.361 | 0.213 | 0.138 |
| L | n/N | | | |
| | 50/10 | 150/10 | 50/40 | 150/40 |
| 5 | 0.002 | 0.001 | 0.000 | 0.000 |
| 11 | 0.377 | 0.376 | 0.063 | 0.076 |
| 15 | 0.855 | 0.850 | 0.641 | 0.636 |
| 21 | 0.910 | 0.904 | 0.920 | 0.921 |
| 25 | 0.907 | 0.905 | 0.931 | 0.927 |
| 31 | 0.910 | 0.907 | 0.934 | 0.937 |
| 35 | 0.914 | 0.909 | 0.937 | 0.940 |

Table 5: Illustrative example. The confidence level of the confidence band is evaluated from 100 repetitions. Data is generated using a Splines basis, and confidence bands are calculated with the Fourier (a) and Legendre (b) families, for several model selection criterion in rows, L in rows and several n and N in columns.

| L | n=150, N=40 |
|---|---|
| L tilde | 0.04 |
| L.CV | 0.04 |

| L | n=150, N=40 |
|---|---|
| L tilde | 0.85 |
| L.CV | 0.26 |

provides wider bands, even though their confidence level is not guaranteed. The method proposed in this paper provides a narrower band with a correct level of confidence. We thus recommend to use the Legendre family with the criteria $\tilde{L}$.



Figure 8: Illustrative example. The confidence level of the confidence band is evaluated from 100 repetitions. Data is generated using a Splines basis, and confidence bands are calculated with the Fourier (a) and Legendre (b) families, for several model selection criterion in rows, L in rows and several n and N in columns.

## 7  Real data analysis

In this section, we illustrate the proposed method on the Berkeley Growth Study data. It consists of the heights in centimeters of 39 boys at 31 ages from 1 to 18. We approximate these curves by the 3 basis Legendre, Splines and Fourier. We select the level of each basis using the method introduced in Section 5.

In Figure 9, we display the confidence bands associated with Section 3 in black and those associated with Section 5, for the three basis. As the data is not periodic, the Fourier basis is meaningless, as is the associated confidence band, whatever the dimension considered. Splines and Legendre basis give similar confidence bands. By analyzing the width of the bands in Table 6, compared to that obtained with $L_{\max}$, we find that they are less smooth but also smaller, and from our empirical study we guess that it makes a trade-off between bias and variance.

23

Figure 9: Real data analysis example. We display the confidence bands for Fourier (left), Legendre (middle) and Splines (right) basis on the Berkeley Growth Study data. Black curves correspond to the confidence bands with $L_{max}$, while colored one are the confidence bands CBE.

Table 6: Real data analysis example, Berkeley Growth Study data. We display the width of the confidence bands for Fourier, Legendre and Splines basis for the confidence band of Section 3 with Lmax and the confidence band of Section 5. We also precise the dimension of the selected model.

|                | Basis | | |
|----------------|----------|---------|---------|
|                | Legendre | Splines | Fourier |
| Width Lmax     | 2.12     | 2.12    | 2.20    |
| Width selected | 1.99     | 1.95    | 2.08    |
| Model selected | 6.00     | 5.00    | 7.00    |

# 8 Conclusion

This paper deals with the construction of confidence bands when considering a functional model. Depending on the nature of the family (an orthogonal or orthonormal basis, or simply a vector space), the theoretical guarantees of the linear estimator are recalled and illustrated. Several confidence bands are then proposed. An extensive experimental study on Fourier, Legendre and Spline basis illustrates the theoretical and methodological propositions, and a real data study is proposed to conclude the paper.

First, when considering a functional family with fixed dimension, we discuss the confidence band derived from Sun and Loader (1994). It is biased if the dimension is not high enough to approximate well the true function. We then propose a new confidence band that corrects this bias. To do this, the bias is estimated and the additional randomness is controlled. A selection criterion is proposed to select the best dimension. Unfortunately, the two types of randomness lead to a wider confidence band, and this result is therefore no more interesting than the naive one, which consists of taking the largest possible dimension $L_{\max}$. Finally, a heuristic selection criterion is proposed to select the dimension on the first confidence band, which has not corrected the bias. It takes into account the bias as well as the variance, to select a moderate dimension. Numerical experiments show that this criterion, combined with the Legendre basis, achieve the best performance when considering the confidence level and the width of the corresponding simultaneous confidence band.

An interesting next step, but out of the scope of this paper, is a theoretical study of this criterion. To our knowledge, there are no results concerning the confidence band with the supremum norm. The euclidean norm has been extensively studied, but is not of interest here, where we want to ensure that the tube is valid as a whole. The supremum norm, on the other hand, is difficult to study theoretically. Futhermore, a keypoint here is the randomness of the criterion, which must also be taken into account, through an oracle inequality for example.

# References

Aneiros, Germán, Silvia Novo, and Philippe Vieu. 2022. "Variable Selection in Functional Regression Models: A Review." *Journal of Multivariate Analysis* 188: 104871.

Basna, Rani, Hiba Nassar, and Krzysztof Podgórski. 2022. "Data Driven Orthogonal Basis Selection for Functional Data Analysis." *Journal of Multivariate Analysis* 189: 104868.

Bunea, Florentina, Andrada E. Ivanescu, and Marten H. Wegkamp. 2011. "Adaptive Inference for the Mean of a Gaussian Process in Functional Data." *Journal of the Royal Statistical Society: Series B (Statistical Methodology)* 73 (4): 531–58.

Chen, Ming, and Qiongxia Song. 2015. "Simultaneous inference of the mean of functional time series." *Electronic Journal of Statistics* 9 (2): 1779–98. https://doi.org/10.1214/15-EJS1052.

Claeskens, G., and I. Van Keilegom. 2003. "Bootstrap Confidence Bands for Regression Curves and Their Derivatives." *Ann. Stat.* 31: 1852–1884".

Diquigiovanni, Jacopo, Matteo Fontana, and Simone Vantini. 2022. "Conformal Prediction Bands for Multivariate Functional Data." *Journal of Multivariate Analysis* 189: 104879.

Goepp, V., O. Bouaziz, and G. Nuel. 2025. "Spline Regression with Automatic Knot Selection." *Computational Statistics and Data Analysis* 202.

Hall, P. 1991. "On Convergence Rates of Suprema." *Probab Theory Related Fields*.

Hernández, Nicolás, Jairo Cugliari, and Julien Jacques. 2024. "Simultaneous Predictive Bands for Functional Time Series Using Minimum Entropy Sets." *Communications in Statistics - Simulation and Computation*, 1–25.

Jacques, Julien, and Sanja Samardžić. 2022. "Analysing Cycling Sensors Data Through Ordinal Logistic Regression with Functional Covariates." *Journal of the Royal Statistical Society Series C:*

562  *Applied Statistics* 71 (4): 969–86.

563  Kokoszka, P., and M. Reimherr. 2017. *Introduction to Functional Data Analysis.* Chapman & Hall /
564  CRC Numerical Analysis and Scientific Computing. CRC Press.

565  Krivobokova, Tatyana, Thomas Kneib, and Gerda Claeskens. 2010. "Simultaneous Confidence Bands
566  for Penalized Spline Estimators." *Journal of the American Statistical Association* 105 (490): 852–63.

567  Lacour, C., P. Massart, and V. Rivoirard. 2017. "Estimator Selection: A New Method with Applications
568  to Kernel Density Estimation." *Sankhya A* 79: 298–335.

569  Li, Yehua, Yumou Qiu, and Yuhang Xu. 2022. "From Multivariate to Functional Data Analysis:
570  Fundamentals, Recent Developments, and Emerging Areas." *Journal of Multivariate Analysis* 188:
571  104806.

572  Liebl, D, and M. Reimherr. 2023. "Fast and Fair Simultaneous Confidence Bands for Functional
573  Parameters." *Journal of the Royal Statistical Society Series B: Statistical Methodology* 85: 842–68.

574  Neumann, M., and J. Polzehl. 1998. "Simultaneous Bootstrap Confidence Bands in Nonparametric
575  Regression." *J Nonparametr Statist* 9: 307–33.

576  Quinton, J-C., E. Devijver, A. Leclercq-Samson, and A. Smeding. 2017. "Functional Mixed Effect
577  Models for Mouse-Tracking Data in Social Cognition." In *ESCON Transfer of Knowledge Conference,*
578  *Gdansk, Polland.*

579  Sachs, Michael C., Adam Brand, and Erin E. Gabriel. 2022. "Confidence Bands in Survival Analysis."
580  *The British Journal of Cancer. Supplement* 127: 1636–41.

581  Sun, Jiayang, and Clive R. Loader. 1994. "Simultaneous Confidence Bands for Linear Regression and
582  Smoothing." *Ann. Statist.* 22 (3): 1328–45.

583  Telschow, Fabian J. E., Dan Cheng, Pratyush Pranav, and Armin Schwartzman. 2023. "Estimation
584  of expected Euler characteristic curves of nonstationary smooth random fields." *The Annals of*
585  *Statistics* 51 (5): 2272–97.

586  Telschow, Fabian J. E., and Armin Schwartzman. 2022. "Simultaneous Confidence Bands for Func-
587  tional Data Using the Gaussian Kinematic Formula." *Journal of Statistical Planning and Inference*
588  216: 70–94.

589  Wang, L. And Yang, J. And Gu. 2022. "Oracle-Efficient Estimation for Functional Data Error Dis-
590  tribution with Simultaneous Confidence Band." *Computational Statistics & Data Analysis* 167:
591  107363.

592  Xia, Y. 1998. "Bias-Corrected Confidence Bands in Nonparametric Regression." *J.R. Stat. Soc. Ser. B*
593  60: 797–811.

594  Zhang, C. And Wu, Y. And Wang. 2020. "Prediction of Working Memory Ability Based on EEG by
595  Functional Data Analysis." *J Neur. Meth.* 333: 108552.

596  Zhou, S., X. Shen, and D. A. Wolfe. 1998. "Local Asymptotics for Regression Splines and Confidence
597  Regions." *Ann. Statist.* 26: 1760–82.

# 9 Appendix: proofs

## 9.1 Proof of Proposition 2.3

Let us prove the first point. We have

$$\mathbb{E}(\hat{\underline{\mu}}^{L,L^\star}) = (\mathbf{B}_L^T\mathbf{B}_L)^{-1}\mathbf{B}_L^T\mathbb{E}(\mathbf{y}) = (\mathbf{B}_L^T\mathbf{B}_L)^{-1}\mathbf{B}_L^T\mathbf{B}_{L^\star}\mu^{L^\star} =: \underline{\mu}^{L,L^\star}.$$

The theory of the linear model gives that the variance of $\hat{\underline{\mu}}^L$ is equal to $\sigma^2(\mathbf{B}^T\mathbf{B})^{-1}\mathbf{B}^T\Sigma\mathbf{B}(\mathbf{B}^T\mathbf{B})^{-1}$ with $\Sigma = Diag(\Sigma_1,\ldots,\Sigma_N)$ the $nN \times nN$ covariance matrix of $\mathbf{y}$. So finally, we have

$$\hat{\underline{\mu}}^{L,L^\star} \sim \mathcal{N}\left(\underline{\mu}^{L,L^\star}, \sigma^2\Sigma_B^{L,L^\varepsilon}\right).$$

26

603 Now we can easily deduce the distribution of $\hat{\underline{f}}^{L,L^*}(t)$, for each $t \in [0,1]$:

$$\hat{\underline{f}}^{L,L^*}(t) - \mathbf{f}^{L,L^*}(t) \sim \mathcal{N}\left(0, \sigma^2 B(t)\Sigma_B^{L,L^\varepsilon}B(t)^T\right).$$

604 To prove that $(\hat{\underline{f}}^{L,L^*} - f^{L,L^*})()$ is a Gaussian process, we consider any finite sequence of times,

605 $(t_1,\dots,t_d) \in [0,1]$. The sequence $(\hat{\underline{f}}^{L,L^*}(t_1) - f^{L,L^*}(t_1),\dots,\hat{\underline{f}}^{L,L^*}(t_d) - f^{L,L^*}(t_d))$ is Gaussian, centered

606 and the covariance is equal to $cov(\hat{\underline{f}}^{L,L^*}(t_1) - f^{L,L^*}(t_1), \hat{\underline{f}}^{L,L^*}(t_2) - f^{L,L^*}(t_2)) = \sigma^2 B(t_1)\Sigma_B^{L,L^\varepsilon}B(t_2)^T$. Thus

607 the process is Gaussian.

## 9.2 Proof of Theorem 3.2

609 We have

$$P(\forall t \in [0,1], |\hat{\underline{f}}^{L,L^*}(t) - f^{L,L^*}(t)| \le \hat{d}^L(t)) = P(\forall t \in [0,1], |\hat{\underline{f}}^{L,L^*}(t) - \underline{f}^{L,L^*}(t) + \underline{f}^{L,L^*}(t) - f^{L,L^*}(t)| \le \hat{d}^L(t))$$

610 Set Assumption 1 and Assumption 3 and a probability $\alpha \in [0,1]$. Then, we have,

$$\lim_{n\to+\infty} P(\forall t \in [0,1], |\hat{\underline{f}}^{L,L^*}(t) - f^{L,L^*}(t)| \le \hat{d}^L(t)) = 1 - \alpha$$

611 with $\hat{d}^L(t) = \hat{c}^L\sqrt{\hat{C}_L(t,t)/N}$ and $\hat{c}^L$ defined as the solution of Equation 4.

## 9.3 Proof of Proposition 4.1

613 To simplify the notations, let us denote $a(t) = \underline{f}^{L,L^*}(t) - \hat{\underline{f}}_1^{L,L^*}(t)$ and $b(t) = \underline{f}^{L_{\max},L^*}(t) - \underline{f}^{L,L^*}(t) -$

614 $(\hat{\underline{f}}_2^{L_{\max},L^*}(t) - \hat{\underline{f}}_2^{L,L^*}(t))$. We have

$$P\left(\exists t |a(t) + b(t)| \ge \hat{d}_1^L(t) + \hat{d}_2^{L,L_{\max}}(t)\right) \le P\left(\exists t |a(t)| + |b(t)| \ge \hat{d}_1^L(t) + \hat{d}_2^{L,L_{\max}}(t)\right)$$
$$= P\left(\exists t |a(t)| \ge \hat{d}_1^L(t)\right) P\left(\exists t |b(t)| \ge \hat{d}_2^{L,L_{\max}}(t)\right) = \alpha\beta.$$

615 The last equality holds thanks to the independence of the two sub-samples.

# 10 Appendix: more experiments

617 Proposition 2.1 and Proposition 2.2 are illustrated in Figure 10. The true dimension is $L^* = 11$. Three
618 families are considered, Fourier, Legendre and Splines. The plots display the absolute difference
619 between the coefficients $\mu_\ell^{L^*}$ and the projected coefficients $\mu^{L,L^*}$, for different $\ell$ in x-axis and for
620 different values of $L$ and $n$ in the y-axis, namely a case with $L < L^*$ and two values of $n$: $L = 7, n = 20$
621 and $L = 7, n = 100$; and a case with $L > L^*$ and two values of $n$: $L = 15, n = 20$ and $L = 15, n = 100$.
622 The absolute difference is represented as a gradient of color, this gradient being adapted to each
623 functional family. We can see that as Legendre (resp. Fourier) are orthonormal (resp. orthogonal)
624 families, the differences are close to 0 when $L = 15$, whatever the values of $n$. When $L < L^*$, the
625 difference is close to 0 when $n$ is large. This property does not hold for the spline family, which is
626 not orthogonal.

Figure 10: Illustrative example. The true dimension is 11, we generate the coefficients with three families, Fourier (which is orthogonal), Legendre (which is orthonormal) and the splines (which are not orthogonal wrt the standard scalar product). In the y-axis, two dimensions of the family (7 or 15) and two numbers of timepoints (20 or 100) are compared. We plot in x-axis the value of the absolute difference between the true coefficients and their approximations for the first 7 coefficients of the basis. The color scale is adapted to each functional basis.